[11] M. S. Gillanders, D. D. Krot, P. S. Vijayakumar, A. V. Mason, G. S. Glenn, D. R. Lillington, B. T. Cavicchi, H. T. Yang, and R. K. Ralph, "Production and qualification status of GaAs/Ge top/bottom coplanar contact solar cells," in *Rec. 22nd IEEE Photovoltaic Specialists Conf.* New York: IEEE, 1991, pp. 1469–1473.

[12] M. L. Ristow, J. C. Chen, M. S. Kuryla, and H. F MacMillan, "A high yield manufacturing demonstration for high efficiency GaAs concentrator solar cells," in *Rec. 22nd IEEE Photovoltaic Specialists Conf.* New York: IEEE, 1991, pp. 128–132.

[13] H. A Vander Plas, L. W. James, R. L. Moon and N. J. Nelson, "Performance of AlGaAs/GaAs terrestrial concentrator solar cells," in *Rec. 13th IEEE Photovoltaic Specialists Conf.* New York: IEEE, 1978, pp. 934–940.

[14] L. D. Partain, J. C. Schultz, G. F. Virshu, and M. L. Ristow, "GaInAs/GaAs thermally actuated optical switch," *Appl. Phys. Lett.*, vol. 57, pp. 1840–1842, 1990.

[15] Z.-Q. Fang and D. C. Look, "Excess dark current due to saw damage in semi-insulating GaAs," *J. Electr. Mtls.*, vol. 22, pp. 1361–1363, 1993.

[16] M. Schneider, C. Colvard, K. Alavi, and E. Kohn, in *Proc. Society of Photo-Optical Instrumentation Engineers*, vol. 797, S. D Mukherjee, Ed. Bay Point, FL: SPIE, 1987, pp. 149–155.

[17] B.-C. Chung, C. W. Ford, B. A. Arau, H. C. Hamaker, M. L. Ristow, J. C. Schultz, G. F. Virshup, and J. G. Werthen, "High-efficiency AlGaAs solar cells grown by metalorganic vapor epitaxy," in *Rec. 20th IEEE Photovoltaic Specialists Conf.* New York: IEEE, 1988, pp. 486–490.

[18] J. G. Werthen, G. F. Virshup, C. W. Ford, C. R. Lewis, and H. C. Hamaker, "2 × 2 cm^2 GaAs space solar cells with 21% conversion efficiency (one sun, AM0)," in *Rec. 18th IEEE Photovoltaic Specialists Conf.* New York: IEEE, 1985, pp. 300–303.

[19] M. Ogawa, "Alloying behavior of Ni/Au-Ge films on GaAs," *J. Appl. Phys.*, vol. 51, pp. 406–412, 1980.

[20] V. G. Weizer and N. S. Fatemi, "The interaction of gold with gallium arsenide," *J. Appl. Phys.*, vol. 64, pp. 4618–4623, 1988.

[21] D. C. Miller, "The alloying of gold and gold alloy Ohmic contact metallizations with gallium arsenide," *J. Electrochem. Soc.*, vol. 127, pp. 467–475, 1980.

[22] S. P. Tobin, "Continued development of metallization for GaAs concentrator cells," Sandia National Laboratories, Albuquerque, NM, Rep. SAND88-7033, Nov. 1988, pp. 73–87.

[23] K. A. Bertness, private communication.

[24] B.-C. Chung, J. C. Schultz, H. F. MacMillan, G. F. Virshup, M. L. Ristow, M. Klausmeier-Brown, and L. D. Partain, *High Efficiency, Three Junction Solar Cells For Concentrator Arrays*, Wright Laboratories, Wright-Patterson Air Force Base, Dayton, OH, Rep. WL-TR-91-2018, Mar. 1991, pp. 44–50.

Calculation of Depletion Layer Thickness by Including the Mobile Carriers

Saeed Mohammadi and C. R. Selvakumar

***Abstract*—A useful analytical approximation for depletion layer thickness, which takes into account the effect of mobile carriers under high forward bias is presented. The new expression predicts, in agreement with computer simulations, a significantly smaller depletion layer thickness at high forward bias than that of conventional theory. The results of these effects for heterojunctions shows a less pronounced effect. The model's validity for different forward biases is also illustrated. Finally, the effect of temperature dependence is discussed.**

I. The Model

The simple depletion region approximation is based on a complete neglect of the influence of mobile carriers within the 'depletion layer' [1]. This neglect of mobile carriers gives rise to significant errors in the calculation of electric field; depletion layer thicknesses and associated capacitances and charging constants. The electric field and potential distributions within the depletion layer are significantly affected by mobile carriers, particularly at low and high forward biases.

Depletion layer approximation is typically applied to the calculation of depletion layer thicknesses in reverse bias situations. However, the same expression can be used to calculate approximately the depletion layer thicknesses for small forward voltages. This approximation becomes worse because the presence of large mobile carrier populations within the depletion region is no longer negligible. To show the effect of these mobile carriers, we consider an abrupt PN junction. A generalization of the following analysis of a more general doping profile PN junction, however, is beyond the scope of this paper.

At low forward biases, majority carriers within the depletion region reduce the net charge density. As a result, depletion layer thickness is larger than that predicted by the conventional depletion region model. For high forward biases, however, an injection of minority carriers into the depletion region increases the net charge density and consequently, depletion layer thickness becomes smaller than the value predicted by conventional model. This effect becomes important when the inverse Early effect in narrow-base bipolar transistors is to be considered.

For an abrupt junction, Frederickson and Rabkin [2] showed that the mobile carrier distribution within the depletion layer can be described by an analytical expression which assumes that the carriers drift across the depletion layer at their saturated velocities. Recently, Suzuki and Nakayama [3] showed that this assumption of carriers transiting the depletion layer at their saturated velocity is a good approximation for calculating transit times. Neglecting nonthermal and thermal generation of carriers, the free electron distribution

Manuscript received August 23, 1994; revised August 11, 1995. The review of this brief was arranged by Associate Editor A. H. Marshak. This work is Supported in part by NSERC and MICRONET.

S. Mohammadi is with the Solid State Electronics Lab, Department of Electrical Engineering and Computer Science, University of Michigan, Ann Arbor, MI 48109 USA.

C. R. Selvakumar is with the Department of Electrical and Computer Engineering, University of Waterloo, Waterloo, Ontario, Canada N2L 3G1.

Publisher Item Identifier S 0018-9383(96)00276-6.

$n_p(x)$ inside the ionized P-type 'depletion' region can be written as follows [2]:

$$n_p(x) = n_{ol}e^{-ax(2x_p-x)} + \frac{D_n n_{po}}{v_{sn}L_n}(e^{V_{be}/V_t} - 1) \quad (1)$$

$$\text{where } n_{ol} = N_D e^{-bx_n^2}$$

and x_p and x_n are distances of the depletion layer boundaries from the metallurgical junction (x=0), n_{po} is the thermal equilibrium minority carrier distribution, L_n is the electron diffusion length, V_{be} is the applied bias on the junction and v_{sn} is the absolute magnitude of the electron saturation velocity. The factors a and b are defined as:

$$a = \frac{q^2 N_A}{2\epsilon kT} \quad \text{and} \quad b = \frac{q^2 N_D}{2\epsilon kT}. \quad (2)$$

A similar equation can be written for the holes inside the ionized N region.

Taking into account only the minority carriers, one can replace the net charge in Poisson's equation with the total of ionized charge density and minority carrier concentration since both have the same polarity. The reason for considering only the minority carriers will be discussed below. Assuming $e^{V_{be}/V_t} \gg 1$ for forward biases in (1), one can solve Poisson's equation to derive an expression for electric field as in (3) (see (3) at the bottom of the page).

$erf(jx)$ is the error-function of imaginary variable jx and may be expanded to its Taylor series by:

$$erf(jx) = \frac{2j}{\sqrt{\pi}}(x + \frac{x^3}{3\times 1!} + \frac{x^5}{5\times 2!} + \frac{x^7}{7\times 3!} + ...) . \quad (4)$$

For high forward biases, one can take the first term and ignore the higher order terms. This approximation cannot be done for low forward biases since the term $\sqrt{a}x_p$ depends upon applied bias and increases as the applied voltage decreases. The reason for considering only minority carriers is now obvious; the minority carriers are too small at low forward biases to introduce any error to error-function approximation. At high applied biases, however, minority carriers cannot be neglected and the approximation is more accurate. By approximating error function to its first Taylor term, one can find a linear approximation model for electric field:

$$E(x) = \frac{q}{\epsilon}\left[N_A + \frac{D_n n_{po}}{v_{sn}L_n}e^{V_{be}/V_t} + n_{ol}e^{-ax_p^2}\right](x_p - x) \quad (5)$$

$$\text{for} \quad 0 < x < x_p \quad .$$

By integrating the electric field, one can find the potential function.

Assuming an N^+P abrupt junction for simplicity and thus neglecting V_n, which is the voltage across the N^+ region, one can find the depletion region width inside the P region as:

$$x_p^2 = \frac{2\epsilon(V_{bi} - V_{be})}{q\left[N_A + N_D e^{(V_{be}-V_{bi})/V_t} + \frac{D_n n_{po}}{v_{sn}L_n}e^{V_{be}/V_t}\right]} . \quad (6)$$

This may be compared with the conventional depletion approximation model:

$$x_p^2 = \frac{2\epsilon(V_{bi} - V_{be})}{qN_A} \quad (7)$$

where V_{bi} is the built-in potential.

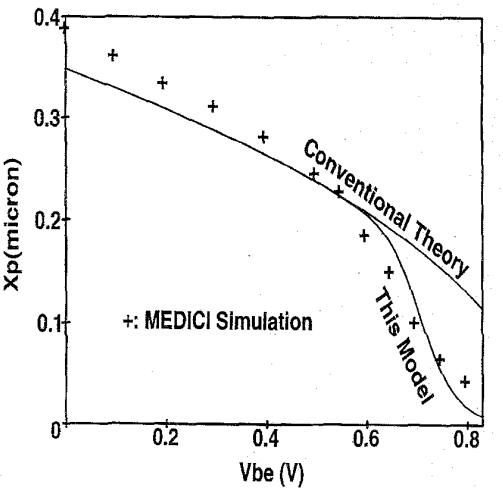

Fig. 1. Comparison of plots of depletion layer thicknesses as functions of forward voltage of an abrupt N^+P junction for $N_A = 1 \times 10^{16}$ cm^{-3}, $N_D = 1 \times 10^{20}$ cm^{-3}, $v_{sn} = 10^7$ cm/s, $\tau_n = 10^{-7}$ s, and $D_n = 31.6$ cm^{2}s^{-1} using conventional theory (7), present analytical model (6), and MEDICI simulations.

II. Discussion and Summary

Fig. 1 depicts the depletion layer width of an N^+P abrupt junction as a function of applied voltage V_{be}. The effect of minority carriers at high forward bias serves to decrease the depletion layer width to less than what is predicted by the conventional model. The difference becomes larger as the ratio between N^+ and P region dopant concentration increases. Also shown in the figure is the result of the MEDICI simulation for the same device. The depletion region boundary is taken to be the point where the electric field becomes 1000 V/cm for numerical expediency.

At high forward biases, our model matches the simulation results with enough accuracy while the conventional model overestimates the depletion layer width. Different electric field profiles inside the P region of the same N^+P abrupt junction for $V_{be} = 0.8$ V are depicted in Fig. 2. As can be seen from the figure, the conventional model profile presents an electric field with a substantially lower magnitude as well as an overestimated depletion layer thickness, while the exact electric field model (3) and the linear approximation model (5) show a close match.

At low forward biases, however, both the conventional model (7) and our model (6) underestimate the depletion layer width as both models ignore majority carriers within the depletion region. Fig. 3 shows such an electric field profile ($V_{be} = 0.4$ V) for the exact electric field model (3) and the conventional model as well as the linear approximation model (5). Although the exact relation (3) shows an electric field with a higher magnitude at the vicinity of the junction, it matches the conventional model and the linear approximation model for larger distances from the junction. Therefore, the approximation is valid for low forward biases since the number of minority carriers at low forward biases is small. Note that, instead of integrating (3), to derive an accurate depletion layer thickness we use (6) as a substitute

$$E(x) = \frac{q}{\epsilon}\left[N_A + \frac{D_n n_{po}}{v_{sn}L_n}e^{V_{be}/V_t}\right](x_p - x) + \frac{q}{\epsilon}n_{ol}\left[\frac{\sqrt{\pi}je^{-ax_p^2}}{2\sqrt{a}}erf(j\sqrt{a}(x - x_p))\right] \quad (3)$$

$$\text{for} \quad 0 < x < x_p \, .$$

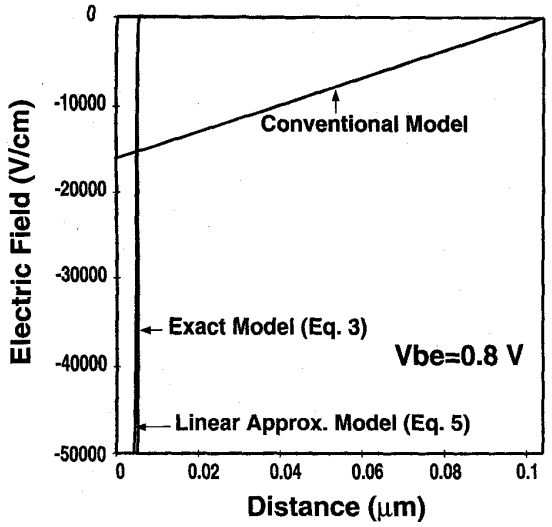

Fig. 2 Electric field profile in P side of the junction for $V_{be} = 0.8$ V for the device of Fig. 1.

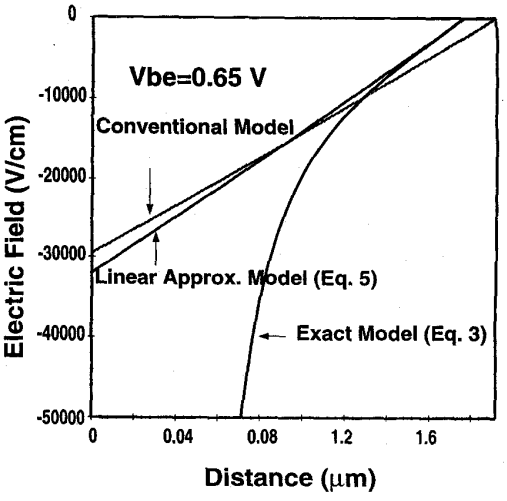

Fig. 4. Electric field profile in P side of the junction for $V_{be} = 0.65$ V for the device of Fig. 1.

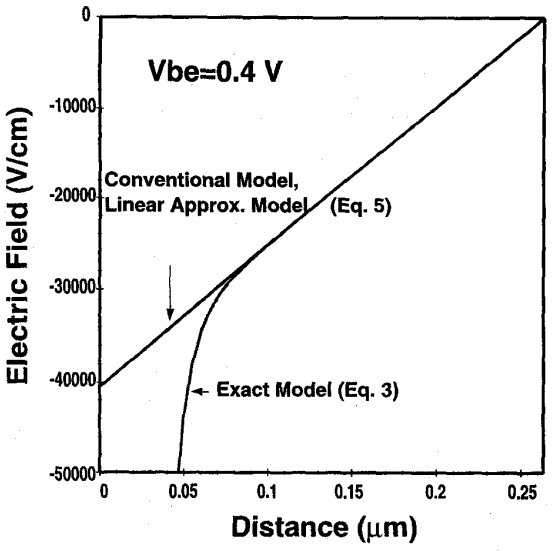

Fig. 3. Electric field profile in P side of the junction for $V_{be} = 0.4$ V for the device of Fig. 1.

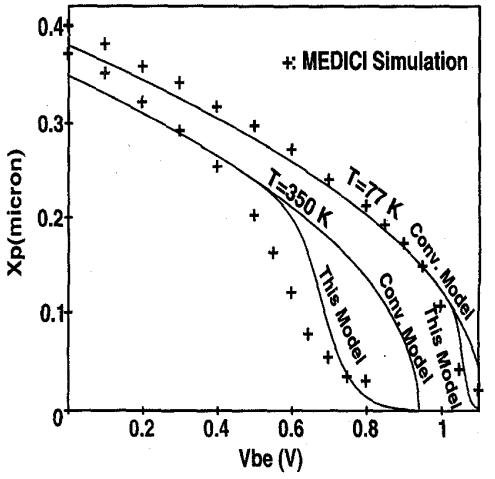

Fig. 5. Comparison of predictions of depletion layer thicknesses as functions of forward voltage shown in Fig. 1 at different temperatures. Diffusion coefficients are calculated from the analytical mobility model with default values given in [4]. The operating temperatures are 77 and 350 Kelvin.

for x_p in (3). Otherwise, the actual junction depth would be smaller, considering only the minority carriers.

At medium forward biases, neither our model nor the conventional model is accurate. This is shown in Fig. 4 where the exact electric field (3) has a substantially different profile than both the conventional and linear approximation models ($V_{be} = 0.65$ V in this case). Since depletion layer thickness for exact electric profile is not known, we used our model (6) to estimate the thickness, however, this is not a good approximation and the actual thickness should be less than what is estimated by our model.

Our model seems to be a good approximation for high forward biases ($\sqrt{a}(x_p) \ll 2\sqrt{6}$) as well as being valid for low forward biases ($n_{ol}e^{-ax_p^2} \ll N_A + \frac{D_n n_{po}}{v_{sn}L_n}e^{V_{be}/V_t}$) while it overestimates the depletion layer thickness for medium forward biases. The presence of majority carriers at medium forward biases compensates for the inaccuracy introduced by our model, therefore, the actual electric field profile derived from the MEDICI simulation is closer to our inaccurate linear approximation at medium forward biases.

Mobile carriers within the depletion region can be neglected for heterojunction devices. In such structures, the region with a larger bandgap is usually doped lower than regular cases while the region with a lower bandgap might be doped higher than a regular case. Thus, the second term in the denominator of (6) can be neglected unlike the first term since the relative difference between the doping of N and P regions is less. The third term in the denominator is also negligible compared to the first term because of the following reasons: for Si/SiGe heterojunctions, the built-in-potential decreases due to a reduction in the bandgap of SiGe material. Since the applied forward voltage is always less than the built-in-potential, it never becomes large enough to increase the third term in the denominator of (6). For GaAs/AlGaAs structures, the built-in-voltage and the

subsequent applied voltage might be high. The number of intrinsic carriers, however, is small and thus the minority carrier equilibrium density n_{po} is small which causes the third term in the denominator of (6) to become negligible.

The effect of temperature on the concentration of mobile carriers within the depletion region might also be of interest. For an N^+P junction, the effect of high temperature (T=350 Kelvin) on the depletion layer thickness on the P side is to accentuate the minority carrier injection into the depletion region of the lower doped p-side and consequently, a higher deviation of depletion thickness from conventional model (see Fig. 5). At low temperatures (T=77 Kelvin), however, the deviation from the conventional model is negligible (also see Fig. 5). Results of the MEDICI simulation are also shown in the figure for comparison. Again, the depletion layer boundary is taken to be the point where the electric field becomes 1000 V/cm.

REFERENCES

[1] D. J. Roulston, *Bipolar Semiconductor Devices*,. New York: McGraw-Hill, 1990.

[2] A.R. Frederickson and P. Rabkin, "Simple model for carrier densities in the depletion region of p-n junctions," *IEEE Trans. Electron Devices*, vol. 40 no. 5, pp. 994-1000, May 1993.

[3] K. Suzuki and N. Nakayama, "Base transit time of shallow base bipolar transistors considering velocity saturation at base-collector junction," *IEEE Trans. Electron Devices*, vol. 39 no. 3, pp. 623-628, Mar. 1992.

[4] *TMA MEDICI* User's Manual, Version 1, vol. 1, Mar. 1992.